

Catalyst-Controlled Aliphatic C–H Oxidations with a Predictive Model for Site-Selectivity

Paul E. Gormisky and M. Christina White*

Department of Chemistry, University of Illinois Urbana–Champaign, Urbana, Illinois 61801, United States

S Supporting Information

ABSTRACT: Selective aliphatic C–H bond oxidations may have a profound impact on synthesis because these bonds exist across all classes of organic molecules. Central to this goal are catalysts with broad substrate scope (small-molecule-like) that predictably enhance or overturn the substrate's inherent reactivity preference for oxidation (enzyme-like). We report a simple small-molecule, non-heme iron catalyst that achieves predictable catalyst-controlled site-selectivity in preparative yields over a range of topologically diverse substrates. A catalyst reactivity model quantitatively correlates the innate physical properties of the substrate to the site-selectivities observed as a function of the catalyst.

Small-molecule catalysis has achieved predictable, substrate-controlled site-selective C–H oxidations with generality and operational ease. We recently described a non-heme iron hydroxylation catalyst, Fe(PDP) (**1**), that showed 3° (tertiary) and 2° (secondary) aliphatic C–H bonds can be preparatively differentiated based on electronic (favors electron-rich sites), steric (favors unhindered sites), and stereoelectronic factors (favors sites where strain relief is possible) that distinguish C–H bonds from one another within a molecule.¹ Catalyst **1** relies on the constructive combination of these factors to favor a single site of oxidation. While **1** provides good selectivity in many molecules because of the pervasiveness of these inherent reactivity differences among C–H bonds,^{2,3} the substrate ultimately dictates site-selectivity. As a result, site-selectivity suffers when individual factors diverge to favor distinct sites, and modulating the magnitude of selectivity or achieving oxidation at alternate sites is not possible without chemically changing the substrate (e.g., directed oxidations).⁴

Catalyst-controlled selectivity that enhances or overturns the substrate's inherent selectivity preference is still at the forefront in asymmetric catalysis⁵ and site-selective modification of reactive functionality.⁶ Aliphatic C–H oxidation presents the additional challenge of requiring a catalyst that is reactive enough to oxidize very inert bonds, yet maintains the capacity for its control elements to differentiate the subtle features of bonds ubiquitous within molecules. Catalyst control is a hallmark of enzymatic aliphatic C–H oxidations.⁷ However, despite significant efforts to adopt the enzymatic strategies of utilizing shape⁸ and functional group recognition⁹ elements, efficient and general small-molecule catalyst control has not been achieved. Challenges associated with creating a discrete match between catalyst and substrate have led to extreme catalyst designs—e.g.,

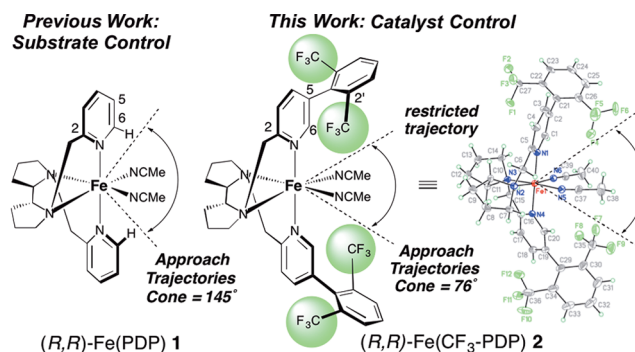


Figure 1. Trajectory Restriction Strategy

complete encapsulation of the active site to select based on substrate topology—thereby limiting the scope to one or a few similar substrates. We describe a small-molecule catalyst that uses a trajectory restriction strategy to achieve predictable, catalyst-controlled site-selectivity while maintaining substrate generality.

In our design strategy, we endeavored to generate a small-molecule catalyst that incorporates minimal steric blocking elements¹⁰ to restrict the approach trajectories of certain C–H bonds to the Fe-oxo (Figure 1). We hypothesized that such a catalyst could alter intrinsic substrate bias by rendering catalyst/substrate nonbonding interactions paramount while maintaining structural flexibility such that substrates of diverse topologies are accommodated. The 3D structure of (R,R)-Fe(PDP) (**1**) reveals a wide 145° cone of possible approach trajectories of a substrate to the putative Fe-oxo so that a combination of electronic and steric/stereoelectronic factors influence site-selectivity variably depending on the substrate. Modifications at the pyridine 6-position of **1** suppressed reactivity, supporting reports that catalysts with steric hindrance near the oxo exhibit greatly diminished C–H oxidation reactivity.¹¹ We thus synthesized a catalyst with pendant aryl rings at the 5-position having *o*-CF₃ groups. *Ortho*-CF₃ disubstitution is ideal because its electron-withdrawing properties deactivate the ligand toward oxidation and its steric bulk (comparable to isopropyl, but rotationally symmetric¹²) enforces a perpendicular biaryl alignment where the CF₃ groups extend toward the catalyst active site and narrow the cone of possible approach trajectories to 76°.

We first examined the ability of catalyst Fe(CF₃-PDP) (**2**) to alter the intrinsic site-selectivities of oxidation with Fe(PDP) **1** over a topologically diverse selection of substrates (Table 1). Oxidizing linear ester (+)-**3** and *trans*-1,2-dimethylcyclohexane

Received: July 22, 2013

Published: September 10, 2013

Table 1. Catalyst-Controlled Oxidation of Simple Cyclic and Acyclic Molecules

| entry (catalyst) | starting material %RSM | oxidation products % yield ^{a,b} | site-selectivity ^c |
|------------------|-----------------------------|---|-------------------------------|
| | | | |
| 1 (1) | (+)-3 ^{d,e} 16 | (+)-4 41 | 2°:3° 1:1 |
| 2 (2) | 8 | 51 | 4:1 |
| 3 (1) | 6 ^{d,f} 11 | 7 28 | 2°:3° 2:1 |
| 4 (2) | 15 | 8 22 9 29 | 10:1 2:1 |
| 5 (1) | 10 ⁱ 0 | 11 19 | 2°:3° 1:2 |
| 6 (2) | 9 | 12 51 | 2:1 2:1 |
| 7 (1) | (+)-13 ^{a,i} 10 | (+)-14 29 | 2°:3°/1 1:2 |
| 8 (2) | 8 | (+)-15 43 | 4:1 1:2 |
| 9 (1) | (+)-16 ^{a,i} 32 | (+)-17 24 | 2°:3°/1 1:1 |
| 10 (2) | 8 | (+)-18 51 | 9:1 6 |

^aAverage of 3 runs. SD = 1–4%. ^bIsolated yields. ^cCrude GC ratio; no change after each addition. ^dMethod A: iterative addition of 5% Fe catalyst, AcOH (0.5 equiv), H₂O₂ (1.2 equiv), MeCN. ^eStarting material recycled x1. ^fGC yield. ^gIncludes 6% 3β-hydroxy product. ^hIncludes 5% 2α-hydroxy product. ⁱMethod B: AcOH (0.5 equiv), MeCN, slow addition of 25% Fe catalyst and H₂O₂ (5.0 equiv) over 1h. ^j¹H NMR ratio. Ns=4-nitrobenzenesulfonyl. Val=L-valine. Nva=L-norvaline.

(6) previously provided poor to moderate selectivity between competing 2° (sterically more accessible) and 3° (more electron rich) sites based on substrate control (entries 1 and 3). In contrast, (*S,S*)-2 diverts reactivity toward the electronically disfavored 2° sites by restricting access of the 3° sites to the oxidant. The substantial improvement in site-selectivity with 2 (entries 2 and 4) affords useful levels of 2° oxidation products (51% yield, 70% yield). In addition to enhancing selectivity in previously poorly selective reactions, we questioned if 2 can also completely overturn the substrate's inherent selectivity to favor an alternate site. Oxidizing *trans*-4-methylcyclohexyl acetate (10) with (*S,S*)-1 provides selectivity for C4 oxidation based primarily on electronics to afford alcohol 12 in 66% yield (entry 5). (*S,S*)-2 overturns this selectivity by exploiting a significant catalyst/substrate repulsive nonbonding interaction with the C4 axial 3° C-H bond and affords good yields (51%) of product at the electronically deactivated C3/5 site (entry 6). Significantly, the same effect is observed with a topologically distinct (acyclic) and functionally dense isoleucine substrate, (+)-13. Oxidation with (*R,R*)-1 affords 43% of alcohol (+)-15 as the major product (1:2

2°:3°, entry 7), whereas (*R,R*)-2 leads to a turnover of site-selectivity affording the methylene oxidation product, γ -ketone (+)-14, in a preparatively useful 56% yield (4:1 2°:3°, entry 8). Catalyst-controlled reactivity can further be applied in a more complex dipeptide setting. While (*R,R*)-1 affords no selectivity for oxidizing (+)-16 due to competing electronic and steric effects (1:1 2°:3°, entry 9), (*R,R*)-2 provides 51% yield of norvaline oxidation with excellent 9:1 2°:3° selectivity (entry 10). In contrast to 1 whose selectivities are dictated by the interplay of electronic and sterics/stereoelectronics *within the substrate*, 2 relies primarily on nonbonding interactions *between the catalyst and the substrate* to control site-selectivities. Significantly, 2 affects changes in site-selectivity relative to 1 under a uniform set of simple reaction conditions (room temperature, open to air, 0.16 M) in preparatively useful yields (ca. 54% isolated yield, mono-oxidized product).

To broadly impact synthetic strategy, catalysts that exert control on site-selectivities of oxidation must do so in a *predictable* way on a diverse range of complex molecules.² We thus developed structure-based catalyst reactivity models that enable systematic identification of the most likely sites of oxidation on a molecule and then quantitative description and prediction of the site-selectivity afforded by each catalyst. To simplify the analysis of complex molecules with many potential sites of oxidation, we developed a *site filter* that identifies likely sites of oxidation based on parameterizations of electronic [E = NPA charges] and steric/stereoelectronics [S , assigned based on Winstein–Holness values (“A values”),¹⁴ Figure 2].^{15,16} These values were systematically categorized across all substrates; only sites with either two red (highly reactive) or one red and one purple (moderately reactive) parameter are considered susceptible to oxidation.

We next sought to develop a model that mathematically relates each catalyst's site-selectivities to the properties of the substrate. We hypothesized that the difference in electronics ($\Delta E_{ab} = E_b - E_a$) and sterics/stereoelectronics ($\Delta S_{ab} = S_b - S_a$), describing the relative reactivity between the sites identified using the site filter (a and b), could be proportional to the experimentally determined site-selectivities (a:b)¹ expressed as a difference in transition-state energies ($\Delta\Delta G^\ddagger \approx 1.36 \log(a:b)$). These data

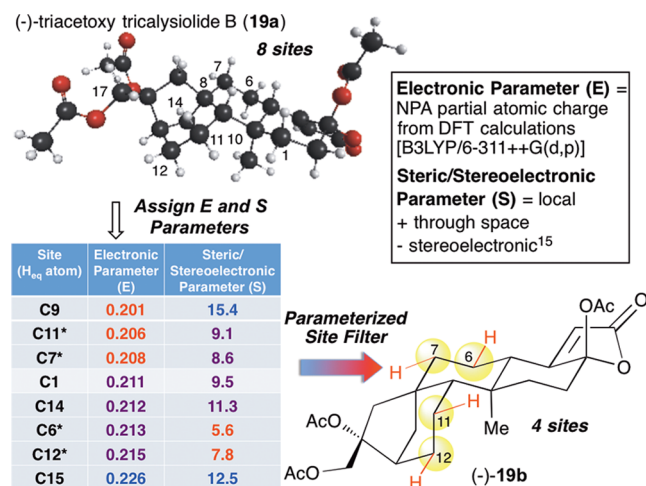


Figure 2. Parameterized site filter for complex substrates. Larger E = more positive charge, more electron poor. Larger S = more sterically hindered. Red = highly reactive (from lowest E up to a 5% increase; from lowest S up to a 40% increase); purple = moderately reactive (from the upper limit of the red region up to a 5% increase (E) or 40% increase (S)); blue = unreactive (anything above the upper limit of the purple region). Acetate substituted sites were excluded from analysis.¹⁵

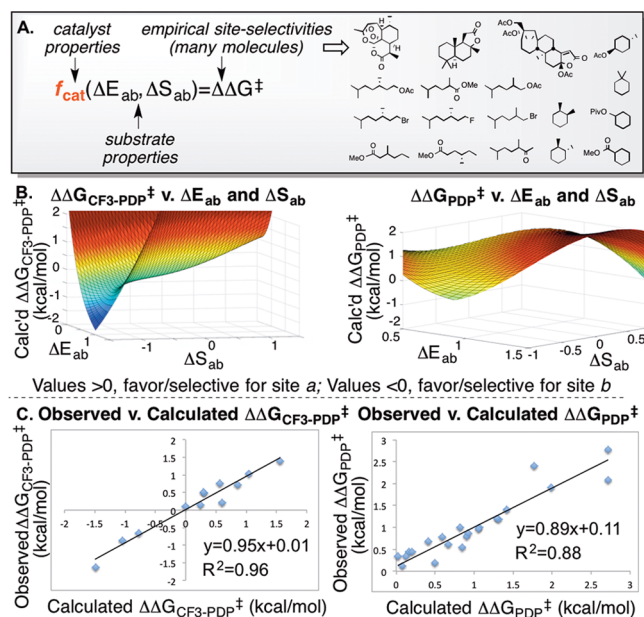
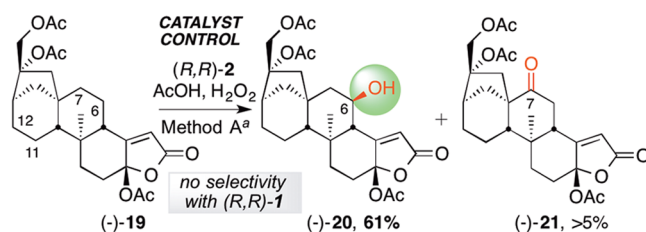


Figure 3. Structure-based Catalyst Reactivity Models

we fit as a function of catalyst $f_{\text{cat}}(\Delta E_{\text{ab}}, \Delta S_{\text{ab}}) = \Delta \Delta G^\ddagger$ to obtain a 3D free energy relationship¹⁷ expressed by an equation for each catalyst (Figure 3A,B).¹⁵ In examining the surface for oxidations with **2**, site-selectivity (i.e., $\Delta \Delta G^\ddagger$, Z-axis) correlates strongly with ΔS_{ab} and is highest when there is a large difference in sterics/stereoelectronics between two sites (ΔS_{ab}) in either direction: the difference in electronics (ΔE_{ab}) can be negligible or even large in the opposite direction. The correlations expressed computationally are fully consistent with the empirical observation that **2** induces catalyst-controlled changes in $\Delta \Delta G^\ddagger$ as a result of nonbonding catalyst/substrate interactions. In contrast, the surface for oxidations with **1** predicts that site-selectivity is highest when electronic and steric/stereoelectronic differences between two sites are large in the same direction. This mathematically expresses the empirical observation that oxidations with **1** are controlled by the confluence of favorable steric/stereoelectronic and electronic properties within the substrate. Comparing the calculated and experimental $\Delta \Delta G^\ddagger$ values for **2** and **1** for all substrates used to create the models provides a good linear fit (Figure 3C). In addition to validating our hypothesis¹ that the basic physical organic parameters of electronics and sterics/stereoelectronics of a substrate correlate to site-selectivities in C-H oxidation, this finding demonstrates for the first time that this relationship can be expressed quantitatively and varied based on catalyst structure.

Next we evaluated the scope of **2**'s ability to alter intrinsic site-selectivities in complex molecule settings as well as the capacity for the catalyst reactivity models to describe the divergent selectivities. Applying the parametrized site filter to (–)-triacetoxytricalysiolide B (**19**), a putative metabolite of the diterpene cafestol found in coffee¹⁸ having eight potential sites of oxidation, revealed four likely sites of oxidation: C6, C7, C11, and C12 (Figures 2 and 4). Evaluating the electronic and steric difference parameters between these sites indicates that the selectivity factors are in opposition; there is a strong steric preference for C6 and an electronic preference for C7 and C11 (Figure 4). Using C6 as our reference in **1**'s reactivity model, we calculate site-selectivity ratios of 1:1.1 (C6:C7), 1:1.4 (C6:C11), and 4:1 (C6:C12), due to these divergent factors within the substrate. The calculated values are consistent with the experimental



Data for (–)-19^b

| Sites (a:b) | ΔE_{ab} | ΔS_{ab} |
|-------------|------------------------|------------------------|
| C6:C7 | -0.35 | 1.09 |
| C6:C11 | -0.48 | 1.27 |
| C6:C12 | 0.11 | 1.28 |

Input into Structure-Based Reactivity Model

| Results for Catalysts 1 and 2 | | | |
|-------------------------------|--|--------------|----------------|
| C6:C7 | calc'd $\Delta \Delta G^\ddagger$ (kcal/mol) | Calc'd Ratio | Observed Ratio |
| cat. 2 | 1.4 | 11:1 | >10:1 |
| cat. 1 | -0.1 | 1:1 | 1:1 |

Figure 4. Influencing site-selectivity in a non-selective C-H oxidation. ^aAverage of 3 runs, SD=3%. Starting material recycled x1. ^bPositive values indicate the parameter favors site a; negative values indicate the parameter favors site b.

findings that oxidizing (–)-**19** with (*R,R*)-**1** furnishes (–)-6 β -hydroxy-triacetoxytricalysiolide B (**20**) in 26% yield and (–)-7-oxo-triacetoxytricalysiolide B (**21**) in 18% yield with no site-selectivity (1:1 C6:C7) and poor mass balance, suggesting unselective oxidation at other activated sites (10% recovered starting material). In contrast, **2**'s reactivity model calculates an 11:1 C6:C7 ratio with higher mass balance due to **2**'s ability to respond to large steric/stereoelectronics ($\Delta S_{6,7} = 1.09$, $\Delta S_{6,11} = 1.28$, $\Delta S_{6,12} = 1.28$). Experimentally, oxidizing (–)-**19** with (*R,R*)-**2** affords (–)-**20** in a 61% isolated yield with a significant catalyst-dependent increase in site-selectivity of C6:C7 oxidation from 1:1 to >10:1 (Figure 4). Interestingly, steric hindrance of the axial hydrogen at C6 retards overoxidation of the alcohol to the ketone by both **1** and **2**. It is notable that excellent enhancement of site-selectivity for C6 oxidation is observed with **2** despite opposing electronics favoring C7.

The greatest challenge for catalyst control is to override the inherent site-selectivity of oxidation to favor an alternate site. Catalyst **2** achieved this in oxidizing simple substrates **10** and (+)-**13**, and we sought to further challenge **2** in a complex molecule setting. Applying our site filter to (+)-artemisinin (**22**)—having nine potential sites of oxidation—eliminates all but C10 and C9 based on very unfavorable electronics and/or sterics at alternate sites. Catalyst **1** is calculated to give a 1.3:1 C10:C9 ratio because it responds to the divergent substrate biasing factors: a strong electronic preference for 3^o oxidation at C10 ($\Delta E_{10,9} = 1.48$) and an opposing steric preference for 2^o oxidation at C9 ($\Delta S_{10,9} = -1.70$).¹⁵ Consistent with this, oxidizing (+)-**22** with (*S,S*)-**1** afforded 54% yield of (+)-10 β -hydroxy-artemisinin (**24**) with 23% yield of (+)-9-oxo-artemisinin (**23**) in a useful 2:1 C10:C9 selectivity^{1a} (Figure 5). Despite the substrate's strong electronic bias favoring C10, the reactivity model for **2** calculates a 17:1 ratio favoring C9 oxidation based on the large steric difference parameter. This may be understood based on **2**'s ability to exploit nonbonding interactions between its biaryl ligand and the substrate's rigid lactone ring system to restrict approach trajectories of the electron-rich C10 C-H bond to the Fe-oxo. Gratifyingly, (*S,S*)-**2** dramatically turns over the substrate controlled selectivity seen with (*S,S*)-**1**, oxidizing at the C9 site in an 11:1 C9:C10 ratio and furnishing 52% yield of (+)-**23**. Catalyst **2**'s ability to override strong electronic substrate bias is analogous to what was observed with **19**, but on a topologically distinct structure. Notably, previous to this work, only P-450 enzymes evolved in the laboratory specifically for the oxidation of (+)-**22** provided comparable levels of selectivity for C9,¹⁹ highlighting the power

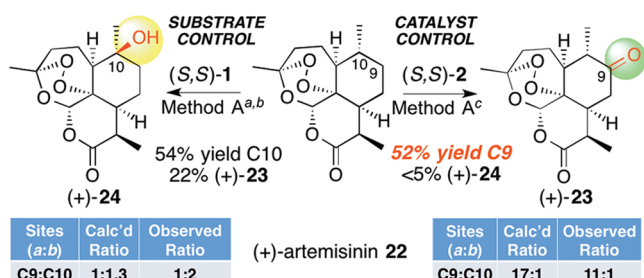


Figure 5. Overriding inherent site-selectivity of C-H oxidation. ^aAverage of 3 runs. ^bStarting material recycled x2. ^cStarting material recycled x4. SD=2%.

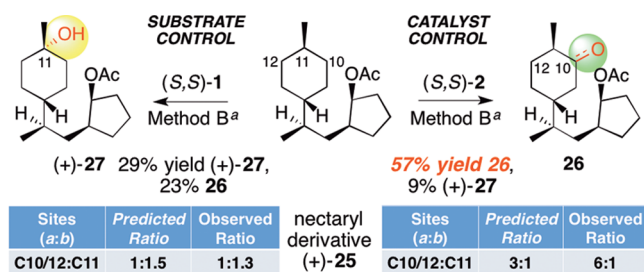


Figure 6. Predictably altering inherent site-selectivity of C-H oxidation. ^aAverage of 3 runs. Starting material recycled x1. SD=3%. 3:1 ketone:alcohol ratio for 26.

of 2 to access new sites of reactivity without the need for substrate specificity.

Models for 1 and 2 are supported by empirical data for substrates incorporated into the original data sets. We next sought to test the predictive power of these models for (+)-nectaryl derivative 25, a synthetic terpene-like molecule used in commercial fragrances that had not been included in the data sets for either catalyst. Applying our site filter, many likely sites of oxidation remained (C11, C10/12, C9/13, C8, C7 and C3): the conformational flexibility of (+)-25 and electronic similarity of its sites made selective oxidation with either catalyst a challenging prospect. Applying the catalyst reactivity models, oxidation of (+)-25 was predicted to modestly favor the more electron rich, 3° C11 site (1.5:1) for 1 and the least sterically encumbered C10/12 site (3:1) for 2 (Figure 6).¹⁵ Consistent with these calculations, oxidizing (+)-25 with (S,S)-1 affords 29% yield of C11 hydroxyl (+)-27 and 23% yield of the C10/12 ketones 26 with poor selectivity (1.3:1). In contrast, (S,S)-2 is able to overcome the electronic substrate bias to furnish C10/12 oxidation products 26 in a 52% yield with good selectivity (6:1). This example illustrates 2's capacity to effect predictable control on site-selectivity based on nonbonding interactions, even in complex substrates with high degrees of conformational flexibility. The site-selectivity models for 1 and 2 are validated as predictive tools, particularly for substrates whose electronic, steric, and stereoelectronic features are well represented by the substrates incorporated into the original data sets.

We show that catalyst control of site-selectivity in aliphatic C-H oxidations is possible—despite the significant challenges associated with controlling highly reactive intermediates—without needing a specific match between one catalyst and one substrate. The development of quantitative structure-based catalyst reactivity models will lead to more targeted application of C-H oxidations at late stages of complex molecule synthesis²⁰ and enable site-divergent diversification of bioactive molecules. The discovery that site-selectivities of oxidation can be mathematically correlated to substrate properties as a function of the catalyst should inform and inspire future catalyst designs.

■ ASSOCIATED CONTENT

Supporting Information

Experimental procedures and characterization data. This material is available free of charge via the Internet at <http://pubs.acs.org>.

■ AUTHOR INFORMATION

Corresponding Author

white@scs.uiuc.edu

Notes

The authors declare no competing financial interest.

■ ACKNOWLEDGMENTS

We thank Dr. D. Rogness and G. Snapper for initial amino acid and peptide oxidation studies, Dr. D. Gray for crystallographic analysis of (R,R)-2 and (+)-25, Prof. A. Pfaltz for a gift of Ir catalysts, and Starbucks for coffee grounds. We are grateful to Bristol-Myers Squibb, Amgen, and the University of Illinois for financial support. P.E.G. is a NSF Graduate Research Fellow.

■ REFERENCES

- (1) (a) Chen, M. S.; White, M. C. *Science* **2007**, *318*, 783. (b) Chen, M. S.; White, M. C. *Science* **2010**, *327*, 566.
- (2) White, M. C. *Science* **2012**, *335*, 807.
- (3) (a) Litvinas, N. D.; Brodsky, B. H.; Du Bois, J. *Angew. Chem., Int. Ed.* **2009**, *48*, 4513. (b) Liu, W.; Groves, J. T. *J. Am. Chem. Soc.* **2010**, *132*, 12847. (c) Paradine, S. P.; White, M. C. *J. Am. Chem. Soc.* **2012**, *134*, 2036.
- (4) (a) Bigi, M. A.; Reed, S. A.; White, M. C. *J. Am. Chem. Soc.* **2012**, *134*, 9721. (b) Desai, L. V.; Hull, K. L.; Sanford, M. S. *J. Am. Chem. Soc.* **2004**, *126*, 9542. (c) Giri, R.; Chen, X.; Yu, J.-Q. *Angew. Chem., Int. Ed.* **2005**, *44*, 2112. (d) Simmons, E. M.; Hartwig, J. F. *Nature* **2012**, *483*, 70.
- (5) Balskus, E. P.; Jacobsen, E. N. *Science* **2007**, *317*, 1736.
- (6) Lewis, C. A.; Miller, S. J. *Angew. Chem., Int. Ed.* **2006**, *45*, 5616.
- (7) (a) Lewis, J. C.; Coelho, P. S.; Arnold, F. H. *Chem. Soc. Rev.* **2011**, *40*, 2003. (b) Kille, S.; Zilly, F. E.; Acevedo, J. P.; Reetz, M. T. *Nature Chem.* **2011**, *3*, 738.
- (8) (a) Groves, J. T.; Neumann, R. *J. Am. Chem. Soc.* **1989**, *111*, 2900. (b) Cook, B. R.; Reinert, T. J.; Suslick, K. S. *J. Am. Chem. Soc.* **1986**, *108*, 7281. (c) Breslow, R.; Huang, Y.; Zhang, X.; Yang, Y. *Proc. Natl. Acad. Sci. U.S.A.* **1997**, *94*, 11156.
- (9) Das, S.; Incarvito, C. D.; Crabtree, R. H.; Brudvig, G. W. *Science* **2006**, *312*, 1941.
- (10) Zhang, W.; Loebach, J. L.; Wilson, S. R.; Jacobsen, E. N. *J. Am. Chem. Soc.* **1990**, *112*, 2801.
- (11) Suzuki, K.; Oldenburg, P. D.; Que, L., Jr. *Angew. Chem., Int. Ed.* **2008**, *47*, 1887.
- (12) Leroux, F. *ChemBioChem* **2004**, *5*, 644.
- (13) For a catalyst with comparable methylene selectivities, but diminished yields and mass balance relative to Fe(PDP): Prat, I.; Gomez, L.; Canta, M.; Ribas, X.; Costas, M. *Chem.—Eur. J.* **2013**, *19*, 1908.
- (14) Winstein, S.; Holness, N. J. *J. Am. Chem. Soc.* **1955**, *77*, 5562.
- (15) For complete details, see SI.
- (16) (a) *Molecular Operating Environment (MOE)*, 2011.10; Chemical Computing Group Inc.: Montreal, 2011. (b) *Gaussian 09*, Revision B.01; Gaussian, Inc.: Wallingford, CT, 2010.
- (17) Harper, K. C.; Sigman, M. S. *Science* **2011**, *333*, 1875.
- (18) Bigi, M. A.; Liu, P.; Zou, L.; Houk, K. N.; White, M. C. *Synlett* **2012**, *23*, 2768.
- (19) Zhang, K.; Shafer, B. M.; Demars, M. D. M., II; Stern, H. A.; Fasan, R. *J. Am. Chem. Soc.* **2012**, *134*, 18695.
- (20) (a) Fraunhofer, K. J.; Bachovchin, D. A.; White, M. C. *Org. Lett.* **2005**, *7*, 223. (b) Stang, E. M.; White, M. C. *Nat. Chem.* **2009**, *1*, 547. (c) McMurray, L.; O'Hara, F.; Gaunt, M. J. *Chem. Soc. Rev.* **2011**, *40*, 1885.